



## Research paper

# Experimental study on human evacuation onboard passenger ships considering heeling angle and opposite directions

Siming Fang<sup>a,b</sup>, Zhengjiang Liu<sup>a,b</sup>, Xinjian Wang<sup>a,b,c,g,\*</sup>, Ben Matellini<sup>c</sup>, Jin Wang<sup>c</sup>, Zaili Yang<sup>c,d,\*\*</sup>, Xinyu Zhang<sup>a,e</sup>, Bo Wan<sup>f</sup>, Shengke Ni<sup>a,b</sup>

<sup>a</sup> Navigation College, Dalian Maritime University, Dalian, 116026, PR China

<sup>b</sup> Key Laboratory of Navigation Safety Guarantee of Liaoning Province, Dalian, 116026, PR China

<sup>c</sup> Liverpool Logistics, Offshore and Marine (LOOM) Research Institute, Liverpool John Moores University, L3 3AF, UK

<sup>d</sup> Transport Engineering College, Dalian Maritime University, Dalian, 116026, PR China

<sup>e</sup> Key Laboratory of Marine Simulation and Control for Ministry of Communications, Dalian Maritime University, Dalian, 116026, PR China

<sup>f</sup> Division of Marine Engineering Operations, China Classification Society, Beijing, 100007, PR China

<sup>g</sup> Key Laboratory of International Shipping Development and Property Digitization of Hainan Free Trade Port, Hainan Vocational University of Science and Technology, Haikou, 570100, PR China

## ARTICLE INFO

## Keywords:

Maritime safety  
Passenger ships  
Emergency evacuation  
Experimental study  
Heeling ships  
Counterflow experiments

## ABSTRACT

It is crucial to understand the movement characteristics and behaviour of individuals during ship emergencies for successful human evacuation on board ships. This study aimed to analyse the effect of heeling angles on human movement characteristics and comprehensive evacuation efficiency on passenger ships through the development of a new experimental dataset of human evacuation. To achieve this, a series of tests were conducted using an experimental simulator closely resembling the evacuation scenarios recommended by the International Maritime Organization (IMO). It is revealed that a heeling angle significantly reduces both walking and running speeds of participants. Notably, when the heeling angle is 16°, males demonstrated better adaptability as their speed was less affected compared to females. Additionally, height is found to be positively correlated with movement speed across different scenarios. In counter flow tests, a comprehensive evacuation experiment was systematically quantified. The results showed that evacuation time increased with higher heeling angles. Furthermore, participants tended to maintain a larger personal space in a heeling ship, resulting in lower density when the heeling angle reached 16° compared to other scenarios. The outcomes of this study offer valuable insights for validating evacuation models and developing guidelines for human evacuation from passenger ships.

## 1. Introduction

The role of passenger ships in the transportation system goes far beyond conventional travel methods. Functioning as carriers, they provide individuals with a multifaceted leisure and tourism experience that includes dining, accommodations, sightseeing, shopping, and entertainment, thereby gaining popularity in contemporary society (Xin et al., 2024). With the continuous expansion of passenger ship operations, the human safety of ships has gained heightened attention (Arshad et al., 2022; Cao et al., 2023b; Huang et al., 2023; Liu et al., 2022; Valcalda et al., 2022; Wang et al., 2021d; Wang et al., 2020; Xie et al., 2022). Despite numerous community efforts, passenger ship accidents,

such as the shipwrecks involving the “Sewol” and “Costa Concordia”, still occur from time to time (Bartolucci et al., 2021; Kim et al., 2016). To mitigate potential serious consequences, effective evacuation measures have become essential for safeguarding the well-being of individuals in the aftermath of an accident.

Since 1995, the International Maritime Organization (IMO) has advocated the inclusion of evacuation performance analyses in the design phase of passenger and Roll-on Roll-off (Ro-Ro) ships. It has also issued a series of “Guidelines” for human evacuations onboard ships (IMO, 2016). Throughout the ensuing decades, the IMO has continually revised and updated these “Guidelines” to incorporate the latest technology and best practices, all with the goal of ensuring the safety of

\* Corresponding author.

\*\* Corresponding author.

E-mail addresses: [X.Wang1@ljmu.ac.uk](mailto:X.Wang1@ljmu.ac.uk) (X. Wang), [Z.Yang@ljmu.ac.uk](mailto:Z.Yang@ljmu.ac.uk) (Z. Yang).

<https://doi.org/10.1016/j.oceaneng.2024.118256>

Received 23 March 2024; Received in revised form 10 May 2024; Accepted 21 May 2024

Available online 2 June 2024

0029-8018/© 2024 The Authors. Published by Elsevier Ltd. This is an open access article under the CC BY license (<http://creativecommons.org/licenses/by/4.0/>).

individuals during their journeys on passenger ships. However, it is noteworthy that even in the most recent version of the evacuation guidelines, the parameters are predominantly based on land-based evacuation studies and do not sufficiently consider the unique challenges of evacuating people from ships, especially in the context of ship accidents, the location of assembly stations, boarding lifeboats, and other pertinent factors (Cao et al., 2023a; Fang et al., 2023, 2024; Wang et al., 2021b). Ships are particularly vulnerable to heeling or trimming after incidents such as collisions and groundings, presenting a heightened challenge for human evacuation (Chan et al., 2023; Christensen et al., 2022; Kang et al., 2019). Regrettably, the datasets from land-based evacuation studies rarely encompass parameters relevant to heeling and trimming scenarios. Simultaneously, the IMO encourages member states to enhance the analysis of human evacuation onboard ships by collecting and sharing data regarding human behaviour and characteristics observed during evacuations. Therefore, although challenging, it is crucial and beneficial to conduct experiments on the human movement in heeling and trimming scenarios to supplement the dataset related to human evacuation onboard ships (Kimera and Nangolo, 2022; Liu et al., 2023; Rong et al., 2022a; Sun et al., 2018a; Wang et al., 2021c).

Human evacuation activities comprise a complex system that draws knowledge from various fields, including pedestrian dynamics and human psychology (Browne et al., 2021, 2022; Rong et al., 2022b). While some research institutes have conducted experiments employing simulators and actual ships, their focus has mainly been on reporting the motion characteristics of individuals or single columns of pedestrians in different heeling and trimming states, with a primary emphasis on the deceleration of individuals' speeds (Bles et al., 2001b; Kim et al., 2019; Zhang et al., 2017). These studies, though valuable, are evidently insufficient to address the complexities of ship human evacuations comprehensively. In an effort to bridge this research gap, an experimental simulator with adjustable heeling angles was established to conduct a series of experiments involving 50 participants with a new aim to investigate the counterflow effect on evacuation beyond the state of the art. Through video tracking technology, the free walking and running speeds of individuals at varying heeling angles are statistically calculated by analysing their trajectories. Furthermore, to more accurately represent the behavioural responses of people in heeling scenarios, experiments involving pedestrians walking in an opposite direction were also conducted. These additional experiments enabled to understand the characteristics of crowd evacuations in heeling environments, facilitating the quantification of key metrics in the evacuation process, such as the density-time relationship, density-speed relationship, and density-flow relationship. It therefore brings new contributions and insights to the field. It is worth noting that this study closely aligns with the evacuation scenarios suggested in the IMO guidelines, and the results can serve as new valuable data support and a theoretical foundation for future related studies.

The rest of this work is structured as follows. Section 2 reviews human evacuation experiments related to heeling or trimming ships, examining them from two distinct angles: real ship experiments, and experiments conducted on experimental simulators. Section 3 provides a comprehensive description of the experiments, encompassing details regarding the experimental participants, experimental environment, and experimental procedure. Section 4 presents the findings, specifically focusing on the impact of varying heeling angles on human free speed and the dynamics of counterflow evacuation. Finally, the conclusions and limitations of this study are given in Section 5.

## 2. Related work

Currently, experimental research on the impact of heeling and trimming on human evacuation primarily revolves around two approaches: observation during actual ship voyages and controlled experiments conducted on experimental platforms.

Thanks to continuous advancements in shipbuilding technology, the stability of ships during actual navigation has notably improved, particularly in the case of large cruise ships (Eliopoulou et al., 2023; Xie et al., 2020). These vessels are often equipped with stabilizer fins designed to ensure passenger comfort during the voyage. However, there is a scarcity of evacuation data related to ship heeling or trimming, making it challenging to acquire insights into human movement characteristics under such conditions, particularly in a quantitative manner (Shafiee and Animah, 2022; Wang et al., 2023a). If movement speed and time could not be quantified, the effectiveness of any corrective measure will not be evaluated in a cost benefit analysis and its implementation becomes less scientifically verified. As a result, many related studies have concentrated on ship motion at smaller angles of heeling or during ship anchoring, as shown in Table 1. For instance, Wang et al. (2021c) observed and analysed the walking speeds of individuals on an ocean-going teaching and training ship, discovering that the ship's motion had an adverse impact on human walking speeds. Moreover, they noted that individuals situated on higher deck levels experienced more significant reductions in their walking speeds. Researchers from the Australian Maritime Engineering Cooperative Research Center (AME CRC) found that at small trimming angles, individuals' downhill speed along the trimming direction increased, while uphill and heeling had minimal effects on walking speed. However, the walking speed of two individuals side by side was significantly lower than that of a single line of individuals (Brumley and Koss, 1998). Researchers from the Research Institute of Marine Engineering of Japan provided data on human moving speed on actual ships, revealing that the ship's rolling motion led to a roughly 30% decrease in individuals' speed compared to heeling at the same angle. Additionally, they concluded that, in trimming and heeling scenarios, people tend to maintain greater distances from one another, resulting in lower population density (Murayama et al., 2000). Researchers from the Korea Ocean & Maritime University conducted tests to measure individuals' speed during berthing and sailing, finding that the speed during sailing was reduced by 27.2% compared to the berthing phase (Hwang, 2013). Walter et al. (2016, 2019) evaluated the stability of human walking at various trimming and heeling angles, examining their distinct impacts on human walking by testing the distances people covered in defined confined areas. Their findings indicated that heeling ship had a more pronounced effect on human moving speed compared to same trimming angle. Furthermore, Chang et al. (2015) employed wireless three-dimensional accelerometers to collect human movement data before and after boarding the ship. They noted that the force required for each step during the voyage was greater than on land, suggesting that this additional force was likely used to adapt one's gait to the ship's motion.

Due to the safety constraints of real ship experiments, most of these studies primarily investigated human movement characteristics under normal navigation conditions. This approach often resulted in discrete data, with test groups consisting mainly of experienced individuals familiar with the ship environment. To broaden the scope of evacuation experiments and enhance their findings, researchers embarked on a series of controlled experiments by establishing experimental platforms to simulate ship environments (Sun et al., 2018b; Zhang et al., 2017). Sun et al. (2018a) analysed the effects of different trimming and heeling angles on individuals' walking using a double-degree-of-freedom hydraulic corridor simulator. Their findings revealed that, for a given heeling angle, the influence on human walking speed was less pronounced than trimming. Moreover, they observed that when individuals walked along a slope at a trimming angle of less than 10° downhill, their speed exceeded that on a flat surface. Similarly, researchers from the Netherlands Organization for Applied Scientific Research found that individuals walking uphill along a trimming direction were more affected by trimming than those walking downhill by a ship motion simulation cabin (Bles et al., 2001b). They also noted that the ship's rolling motion had an additional impact on walking. Lee et al. (2004) further quantified the relationship between ship motion and the static

**Table 1**  
Comparison of the reviewed studies.

No.	Reference	Experimental facility	Contributions
1	Koss et al. (1997)	Real ship	The speed of individuals going down the slope increased with the rise of the trim angle, while the influence of heeling and uphill on the speeds was not significant, but the speed of two people walking side by side in the trim/heeling ship was further reduced.
2	Murayama et al. (2000)	Corridor simulator/Real ship	Individuals' walking speeds on the corridor and stairs were 1.4 m/s and 0.7 m/s, respectively. These speeds were approximately 70% of that of static inclination of 10° when the rolling and pitch angle is 10°. Individuals wanted to keep a distance from each other and the density was reduced when ship inclined.
3	Bles et al. (2001a)	Ship motion simulation cabin	The influence of uphill on individuals' walking speeds were greater than that of downhill. A certain degree of pitching and rolling can reduce walking speed by 15%. Handrails proved effective in assisting individuals during walking.
4	Lee et al. (2004)	Corridor simulator	Due to psychological factors, individual's downhill speed tended to decrease rather than increase. Natural conditions affecting ship movement resulted in a reduction of individuals' walking speeds by approximately 10%–20%.
5	Hwang (2013)	Real ship	Individuals' walking speeds in corridors during ship navigation were 27.2% slower than those at the berth, and speeds around corners during ship navigation were 23.2% slower than those of ship at the berth. Speeds measured for upward and downward stairs were 0.71 m/s and 0.75 m/s, respectively.
6	Zhang et al. (2017)	Maritime rescue simulator	When angles were small, rolling ships had a negligible impact on individual's behaviour during evacuation. However, as angles increase, individuals tended to adjust their walking speeds to regain equilibrium, and they may pause or even fall if the linear acceleration generated by ship rolling exceeded individuals' tolerable limits.
7	Sun et al. (2018a)	Corridor simulator	When the slope angle was below 10°, individual's walking speed increased due to gravity, with heeling angle having a lesser impact on walking speed compared to same trim angle.
8	Wang et al. (2021c)	Real ship	The rolling angle inversely affected individual's walking speeds, with greater attenuation observed on decks farther from the rolling centre.
9	Azizpour et al. (2022)	Corridor simulator	In heeling scenarios, males exhibited notably better performance than females, while wearing a thermal protective immersion suit reduced individual's walking speed by 29–38%.
10	This study	Verification scenario simulator	The individual's free walking speeds in different heeling scenarios are tested, and the counterflow tests at different heeling angles are carried out.

effects of heeling or trimming on walking by deploying a corridor simulator on a real ship. Their investigations revealed that natural ship motion conditions resulted in an additional reduction in human speed, typically around 10%–20%. In a different approach, Zhang et al. (2017) observed human movement in a rolling environment using a maritime rescue simulator. They discovered that individuals needed to constantly adjust their movements while walking, leading to a reduction in speed. Additionally, Azizpour et al. (2022) focused on the innovative aspect of the impact of wearing thermal protective immersion suits on human movement speed during polar voyages. Their study highlighted the influence of individual parameters such as gender, height, weight, and age on walking speed. Overall, they found a significant decrease in speed of participants, with a reduction of approximately 29%–38% when the trimming angle reached 20°.

While previous studies have actively discussed the effects of heeling and trimming ship on human movement, it is important to note that the experimental conditions in these studies lacked uniform standardization. This resulted in varying levels of participant movement, leading to significant variability in the experimental outcomes. Furthermore, most of these studies primarily concentrated on how ship heeling or trimming affects individual passengers, focusing on their movement speed and characteristics during evacuation, without taking into account the interactions between passengers during the evacuation process. In an effort to overcome the limitations of previous research and provide a more comprehensive understanding, this study conducted a comprehensive evacuation experiment under heeling scenarios and makes the following new contributions.

- 1) The experimental innovation lies in the departure from traditional single-corridor simulators, opting instead for a standard experimental simulator based on IMO recommended scenarios. This strategic choice significantly enhances the accuracy and credibility of the experimental results. The establishment of a standardized experimental simulator ensures the acquisition of comprehensive and reliable datasets, offering an effective validation foundation for future simulations and experiments related to human evacuation on heeling ships.
- 2) The experiment not only tested the free walking and running speeds of 50 participants in various heeling scenarios but also employed video tracking technology for precise quantification of the entire evacuation process. This approach expanded the scope of the experiments beyond single-dimensional indicators like speed and time, allowing for a comprehensive exploration of the complex dynamics involved in the evacuation process. Furthermore, the detailed data collection not only enhances the objectivity and reliability of the experimental results but also furnishes a robust foundation for subsequent in-depth data analysis.
- 3) The counterflow testing was conducted with innovation, meeting the test requirements of IMO recommended scenarios while emphasizing the interactions among participants during evacuation in various heeling scenarios. By excavating the dynamics of human behaviour in specific scenarios, the interaction between individuals, such as avoidance behaviour and coordinated actions, could be more accurately captured. This approach facilitates a comprehensive understanding of how heeling scenarios influence the evacuation process.

### 3. Experiment setting

#### 3.1. Experiment participants

Acquiring an understanding of the fundamental characteristics of human movement in heeling environments is the basis for carrying out human evacuation on heeling ships. To accomplish this, a series of experiments was executed using an adjustable heeling simulator. These experiments were carried out at Dalian Maritime University in June 2023. The experiment took place outdoors, benefiting from favourable

weather conditions. The day of the experiment was marked by clear skies and a comfortable temperature of approximately 20 °C, with no precipitation. These ideal weather conditions provided a suitable environment for the participants, without any atmospheric factors significantly impacting their performance. The experimental procedure was approved by the Human Research Ethics Committee of Dalian Maritime University.

50 participants aged 18–25 were recruited, including 35 males and 15 females. These participants are ordinary people instead of seafarers of intensive training on walk on a heeling or trimming ship. The height and weight of each participant were obtained via a questionnaire, as depicted in Fig. 1. The average height for males is  $1.80 \pm 0.12$  m, and for females, it is  $1.64 \pm 0.06$  m. Similarly, the average weight for males is  $75.2 \pm 34.8$  kg, and for females, it is  $55.9 \pm 14.1$  kg. To ensure the alignment of experimental results with the gender and physical attributes of the participants, each individual was assigned a unique serial number during the experiment. Females were numbered from No.1 to 15, while males were numbered from No.16 to 50. These serial numbers were employed throughout the experiment. All participants were informed about the risks and the fundamental procedures of the experiment.

In addition, careful attention was paid to safeguarding the rights and welfare of participants throughout organization of the experiment. Consequently, following rigorous approval by the Ethics Committee, each participant was offered both accident insurance and basic cash reward. This initiative not only acknowledges their commitment of time and effort but also aims to encourage and support their positive engagement in the experiment. Furthermore, to simulate potential emergency scenarios and motivate participants to complete tasks quickly and accurately, a special reward mechanism was implemented. Participants demonstrating exceptional performance, and efficient completion of evacuation tasks were eligible for additional cash incentives. This incentivization strategy was designed to stimulate participants to react faster in emergency situations, thereby enhancing the authenticity and reliability of the experimental results. Moreover, the experiment manager strictly monitored participants' behaviour throughout the experiment to ensure adherence to experimental requirements and prevent any adverse impact on the research findings.

Due to the possibility of encountering large heeling angles during the experiment, in the formulation of the experimental plan, special consideration was given to ensuring participants' safety. Specifically, when the heeling angle exceeds 15°, participants face significant challenges to their balance, and the slightest misstep in this unstable environment can lead to injuries. Consequently, to maximize the safety of the participants, recruitment focuses exclusively on young individuals.

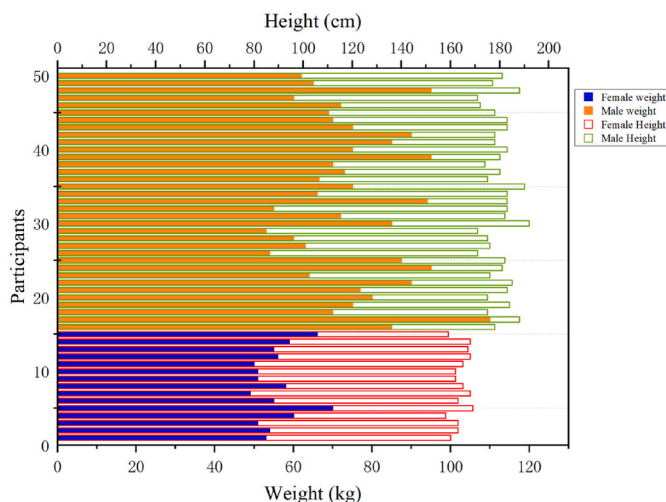


Fig. 1. Height and weight distribution of each participant.

### 3.2. Experiment environment

To analyse human behaviour characteristics during evacuations, the IMO introduced a verification scenario for simulating counterflow. This scenario comprises two rooms measuring 10 m by 10 m each, connected by a 10 m long and 2 m wide corridor, as depicted in Fig. 2. Serving as a verification analysis, this scenario aims to observe human behaviour during simulations. Thus, to establish a standardized experimental environment, an experimental platform based on the recommended IMO test scenario is constructed and human evacuation experiments under heeling conditions are conducted in this study. The objective is to gather detailed test parameters and facilitate quantitative analysis of verification scenarios.

To prioritize participant safety and mitigate the risk of falls resulting from the experimental platform's height differential during large heeling angles, adjustments were made to the experimental platform configuration. These adjustments predominantly involve reducing the recommended scenario size by half, as visually demonstrated in Fig. 3. This proactive measure was implemented to address the heightened risk posed by substantial height differentials, especially in instances of significant heeling angles. The simulator comprises two squares, each with sides measuring 5 m, connected by a 5-m-long and 1-m-wide corridor. Detailed experimental parameters can be found in Fig. 4. To establish the desired heeling angle for the simulator, six adjustment points (highlighted in orange in Fig. 4) were marked by modifying the height of these points to achieve the intended heeling angle.

The experiment took place on an open simulator situated beneath a building. For the experiment, two cameras were employed, each with a resolution of  $1920 \times 1080$  pixels and a frame rate of 25 fps. These cameras were strategically positioned on the fourth floor, 12 m above ground, and the fifth floor, 15 m above ground, of the adjacent building. Importantly, both cameras had the capability to capture the entire experimental area.

### 3.3. Experiment procedure

Given that the platform's heeling angle must be adjusted during the experiment, the position of the corresponding coordinate point in the image will vary, potentially causing distortion in the camera-captured image. Hence, prior to commencing each experiment, the coordinates in the image were marked using a calibration rod.

The primary objective of the experiment is to assess the movement characteristics of individuals in two distinct modes: a free-speed test and a counterflow experiment. The free-speed test involved measuring participants' regular walking and running speeds, while prioritizing safety. To ensure precise tests, the free-speed test area on the simulator was demarcated using highly visible tapes, such as the green dashed zone depicted in Fig. 4 (a). This designated area, measuring 15 m in length and 1 m in width, was positioned at the centre of the connecting corridor. Participants were instructed to confine their movements solely within this marked area. An experiment administrator was stationed at the end of the test zone to closely monitor actions of participants in real time, particularly for any inadvertent deviations or side-slips from the designated area. In cases where a participant inadvertently strayed, they were promptly asked to retest to maintain data accuracy. Furthermore, it is crucial to emphasize that to maintain consistency and standardization in the running behaviour of all participants during the experiment, clear instructions were provided before the experiment. The command of "run" given to the participants during the test is to go through the test area as quickly as possible while prioritizing safety.

In the counterflow experiments, 50 participants were allocated into two groups of randomly mixed participants situated within the waiting areas on the left and right square platforms, as illustrated in Fig. 4 (b). To distinguish between the movements of these two groups, blue hats were provided to those in the left area and red hats to those in the right area. In this experimental setup, participants were instructed to swiftly



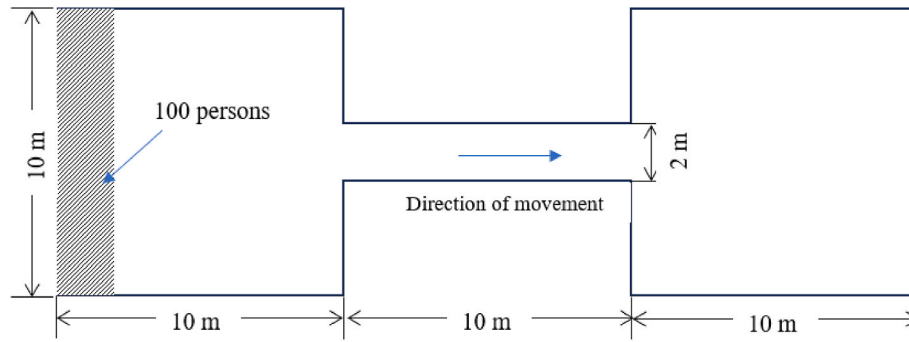


Fig. 2. Verification scenario setting details recommended by IMO.

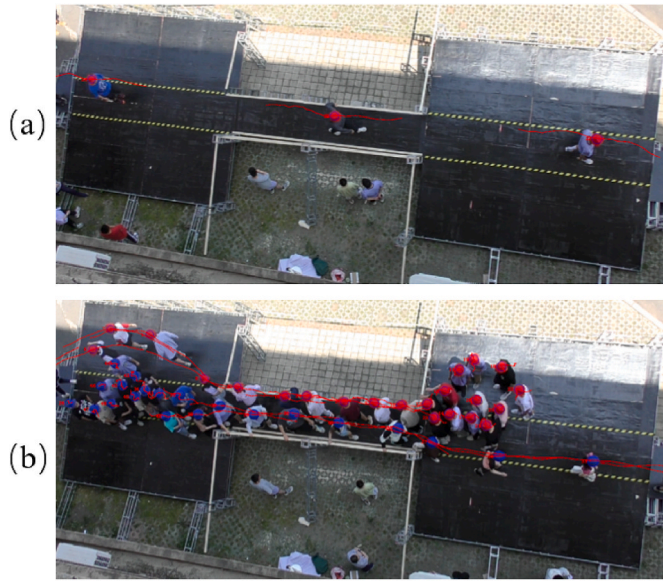


Fig. 3. Snapshots of experiments for (a) walking speed testing and (b) counterflow testing when heeling angle is  $16^\circ$ .

traverse the connecting corridor and reach the opposite end of the experimental simulator. Common understanding dictates that the connecting corridor is a shared pathway for all individuals, potentially leading to the formation of a dense crowd with people moving in opposing directions. As a result, this area was designated as a high-density testing zone to facilitate a more detailed observation and analysis of human movement and behaviour in densely populated scenarios.

## 4. Results and data analysis

### 4.1. Data extraction

Several measures were implemented to monitor the movement trajectories of the experimental participants and minimize experimental errors. Firstly, all participants were required to wear light-coloured clothing and either a red or blue hat. This was done to enhance their visibility in the video recordings, thereby improving the accuracy of the video tracking software, especially in intricate experimental environments.

The Pe-track software was employed to detect and track participant movements, with a sampling rate set at 12 frames/s to capture even the subtlest changes in human motion. Given the complexity of the experimental environment, which encompassed numerous heeling scenarios, a calibration rod was used to record the coordinate parameters of the experimental simulator before the start of each heeling scenario. This precaution allowed us to acquire precise positional data, thus minimizing errors in data extraction.

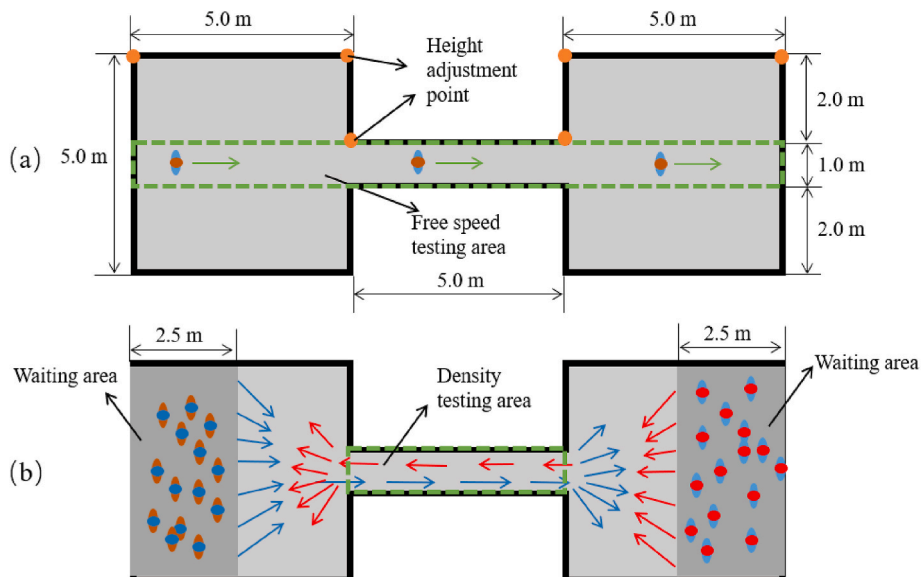


Fig. 4. Schematic diagrams of the experiment: (a) free speed testing and (b) counterflow testing.

Furthermore, during image processing, the calibration rod's position is identified within the Pe-track software to rotate and translate every frame of the photo, thus guaranteeing the vertical alignment of the  $x$ ,  $y$ , and  $z$  axes. The precise calibration parameters can be obtained through Pe-track software, and the detailed calibration parameters are showed in Table 2, including rotation and translation of the  $x$ ,  $y$ , and  $z$  axes. For instance, when the heeling angle is  $0^\circ$ , it's necessary to rotate the  $x$ ,  $y$ , and  $z$  axes of the photo by  $2.754^\circ$ ,  $2.137^\circ$ , and  $-0.323^\circ$  respectively in three-dimensional space, and translate them by  $-1261.6$  mm,  $231.7$  mm, and  $-1895.2$  mm respectively. Meanwhile, to ensure the accuracy and reliability of the data, through exhaustive analysis of the experiment video frame by frame, any abnormal movements are accurately identified, and manual adjustments and calibrations are executed to correct these discrepancies. Moreover, for some abnormal data points that substantially impact the experimental results, a strategy of elimination is employed to avoid their interference with the overall results. The implementation of these measures has significantly enhanced the quality of the experimental data, laying a robust groundwork for subsequent data analysis and conclusions.

#### 4.2. Analysis of free speed

While previous studies have primarily concentrated on the individual movement speeds in heeling environments, the absence of standardized reference values for individuals in such scenarios persists due to variations in experimental settings and participant characteristics. In free-speed tests, the influence of heeling angles on the movement speeds of individuals with varying characteristics was specifically examined. Fig. 5 illustrates the distribution of walking and running speeds among the participants for different heeling angles, with red points representing females and blue points representing males. It is evident that the speed of males significantly exceeds that of females in each heeling scenario in Fig. 5. Furthermore, as the heeling angle gradually increases, both male and female groups exhibit an overall declining trend in their speeds. Of particular note is that, when the heeling angle  $\theta$  reaches  $16^\circ$ , the walking and running speeds of all groups witnessed a notable decrease. However, due to the excellent mobility ability of some male participants, they achieved remarkably high speeds even when faced with a  $16^\circ$  heeling angle, with one instance reaching an outlier speed of  $3.73$  m/s.

To provide a more detailed depiction of the trend in human speed variation, speed reduction factor  $\sigma$  is introduced to analyse the extent of speed reduction in each group.  $\sigma$  is calculated as shown in Equation (1).

$$\sigma = \frac{v_\theta}{v_0} \quad (1)$$

where,  $v_\theta$  is the average velocity of the male and female groups when the heeling angle is  $\theta$  and  $v_0$  indicates the average velocity when no heeling is present.

Fig. 6 illustrates the data for males and females alongside the mean speed reduction factor, revealing a noticeable decrease in walking and running speeds for both genders when  $\theta = 16^\circ$ . In comparison to

scenarios with no heeling, males experience a reduction of 17.7% in walking speeds and 26.1% in running speeds when  $\theta = 16^\circ$ . For females, the reduction is even more pronounced, with walking and running speeds decreasing by 19.9% and 32.6%, respectively. This implies that heeling ships had a more pronounced negative impact on human running speeds. It is worth mentioning that when the heeling angle is  $16^\circ$ , males exhibited slightly lower speed reduction compared to females in both walking and running free speed tests. It is indicated that males in this study may exhibit better adaptability to heeling ships in terms of speed performance. They seem capable of quickly adjusting their body posture to maintain relatively high speeds. In other heeling scenarios, the degree of speed reduction showed little variation between males and females, indicating a relatively balanced effect of the heeling angle on both genders. This observation is consistent with the findings of Sun et al. (2018a). It is essential to emphasize that the study of Sun et al. (2018a) was conducted within a closed corridor simulator, where participants could rely on the simulator's side wall for support while walking. Consequently, it appears that the individuals' average speeds in certain heeling or trimming scenarios exceeding those in flat terrain conditions. However, the environment of this experiment was open, devoid of any walking aids during testing. As a result, there was no phenomenon that the speeds on flat terrain were lower than that on heeling scenarios, which was different from the results obtained by Sun et al. (2018a).

It is well-established that human movement speed typically correlates with an individuals' body size, especially height (Azizpour et al., 2022). In Fig. 7, it is illustrated the connection between participants' walking and running speeds and their heights at various heeling angles. The error bars are determined using the Akima Spline method, and linear regression analysis was conducted on the data points (Wang et al., 2021a). Upon analyzing the fitted data, it becomes evident that human movement speed exhibits a positive correlation with an individual's height. Moreover, the slope of the fitted curve for running speed surpasses that for walking speed. This discrepancy indicates that running speed demonstrates a more pronounced increase in relation to height compared to the walking mode.

The influence of an individual's height on their speed noticeably decreased as the heeling angle gradually increased. In the no-heeling scenario, it can be observed that the disparities in walking and running speeds among individuals of varying heights were  $0.36$  m/s and  $1.39$  m/s, respectively. However, as the heeling angle increased to  $16^\circ$ , these differences reduced to  $0.29$  m/s and  $0.96$  m/s, respectively. It is suggested that the disparities in speeds among individuals of different heights diminish as the heeling angle increases. This trend can be attributed to the notion that the effect of height on speeds becomes more constrained in extreme heeling environments, resulting in a more pronounced limitation on human speed and a subsequent reduction in the height-related impact on speed. These findings deepen the comprehension of the behavioural characteristics of individuals in heeling ships, particularly when height is considered as a contributing factor.

#### 4.3. Analysis of counterflow testing

While individual free movement speeds have been analysed in different heeling scenarios, counterflow experiments have also been carried out to comprehensively evaluate the collective impact of heeling ships on human evacuation. Counterflow is very common in the evacuation process onboard passenger ships. However, in the current literature, the effect of counterflow on the passenger ships' evacuation is at large overlooked. This type of experiment is not only endorsed by the IMO as a recommended test scenario but also facilitates a quantitative assessment of evacuation efficiency by observing individual avoidance behaviours, path selections, and other related behaviours. Consequently, 50 participants were randomly placed in a waiting area on either side of the simulator, with 25 participants in each group. The Heeling angle of the simulator still changed from  $0^\circ$  to  $16^\circ$ .

**Table 2**

Extrinsic parameters for different heeling scenarios.

Heeling angle	Rotation ( $x$ , $y$ , $z$ )	Translation ( $x$ , $y$ , $z$ )
$0^\circ$	( $2.754^\circ$ , $0.137^\circ$ , $-0.323^\circ$ )	( $-1261.6$ mm, $231.7$ mm, $-1895.2$ mm)
$4^\circ$	( $2.742^\circ$ , $0.145^\circ$ , $-0.290^\circ$ )	( $-1223.2$ mm, $263.7$ mm, $-1910.3$ mm)
$8^\circ$	( $2.743^\circ$ , $0.144^\circ$ , $-0.282^\circ$ )	( $-1212.3$ mm, $261.4$ mm, $-1913.0$ mm)
$12^\circ$	( $2.737^\circ$ , $0.185^\circ$ , $-0.331^\circ$ )	( $-1259.7$ mm, $247.2$ mm, $-1896.9$ mm)
$16^\circ$	( $2.796^\circ$ , $0.171^\circ$ , $-0.371^\circ$ )	( $-1272.5$ mm, $187.2$ mm, $-1884.4$ mm)

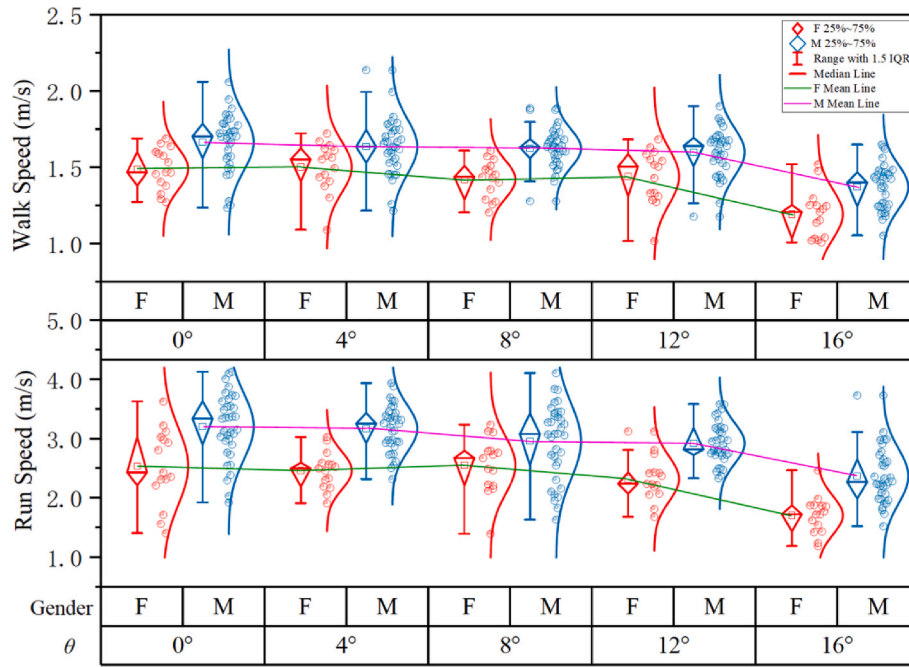


Fig. 5. Box plots of walking speed and running speed for female and male groups.

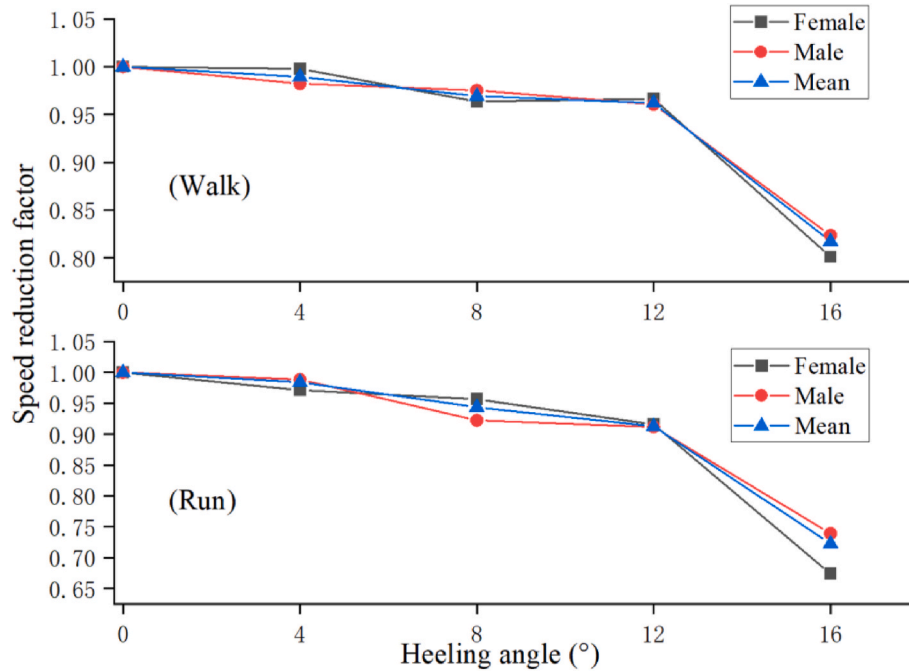


Fig. 6. Speed reduction factors of female and male groups at different heeling angles.

The evacuation trajectories of participants at different heeling angles are presented in Fig. 8. It is noteworthy that participants consistently adhered to the practice of walking on the right in all scenarios, which aligns with findings from previous studies (Yang et al., 2014). Moreover, during the counterflow experiments, it is observed that participants' trajectories often exhibited significant wavering before they entered the corridor. It is suggested that individuals tend to queue up and wait at the corridor entrance before proceeding into the connecting area. This waiting phase led to the congregation of individuals near the corridor entrance, resulting in the observed wobbly trajectories. However, once individuals passed through the corridor, their trajectories became more

linear and smoother, akin to the blue trajectories on the left and the red trajectories on the right in Fig. 8. It is crucial to note that, since specific exits were not designated, participants defaulted to departing the experimental simulator as the end of the experiment. Therefore, trajectories typically exhibited a more dispersed and fluid pattern as people left the simulator. It is worth highlighting that two stair steps were introduced at both the left and right ends of the experimental simulator when  $\theta \geq 12^\circ$  to ensure the safety of participants due to the considerable height difference between the simulator and the ground. This introduction of steps explains the more centralized trajectories observed when participants departed the experimental simulator in scenarios

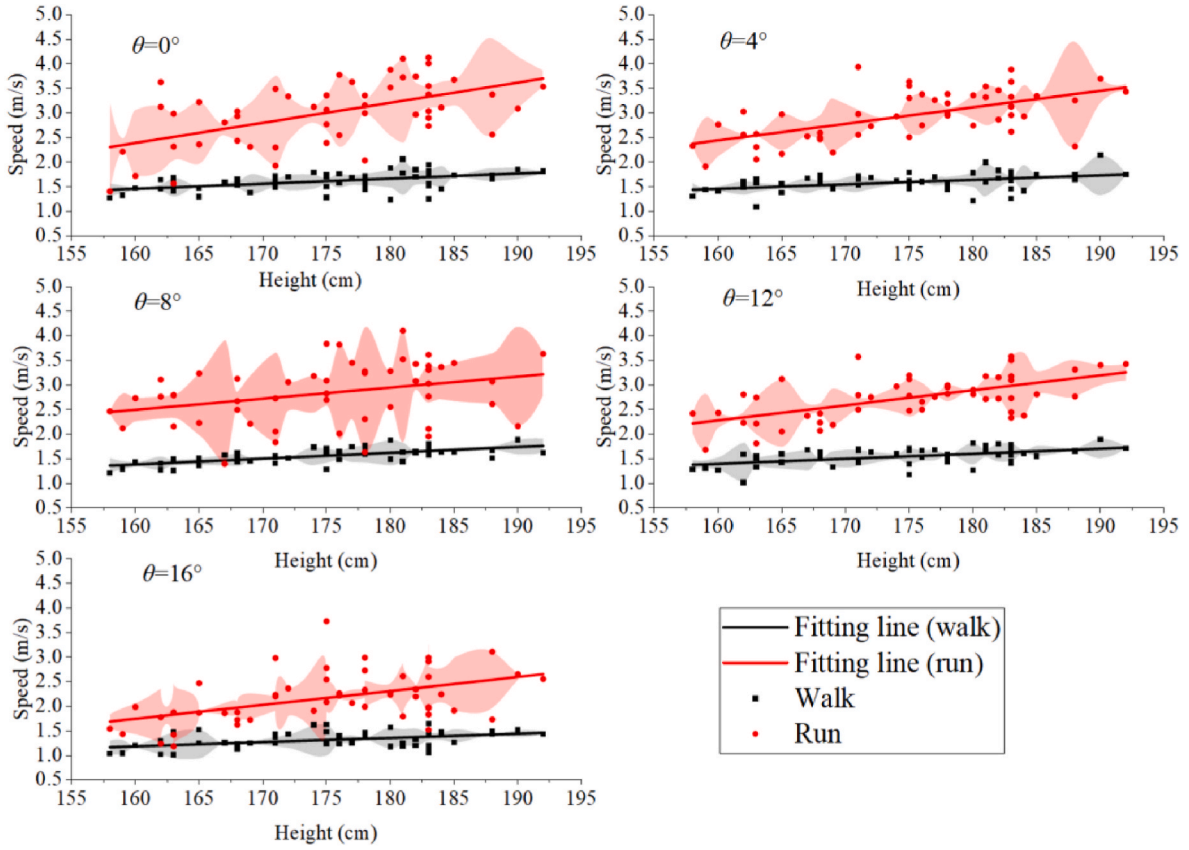


Fig. 7. Walking and running speeds for individuals of varying heights.

with 12° and 16° of heeling angle.

Although 2D trajectories can capture human spatial distribution, it cannot provide a detailed depiction of the evolution of participants' positions over time. Therefore, spatio-temporal trajectories of participants in various heeling scenarios are presented in Fig. 9, red and blue trajectories are employed to illustrate human movement on the two platforms, respectively. It can be clearly seen that the evacuation time required for participants to exit the experimental simulator progressively lengthens with increasing heeling angles in Fig. 9. In the no-heeling scenario, it only took 24.75 s for all participants to complete the evacuation. However, when the heeling angle reached 16°, the total evacuation time extended to 37.83 s, signifying a 52.84% reduction in evacuation speed.

It is important to highlight that, as participants predominantly moved horizontally from left to right (blue trajectories) or right to left (red trajectories), the alterations in the x-axis coordinates of trajectories in Fig. 9 distinctly portray the temporal evolution of human movement. Gentle trajectory segments indicate that individuals covered a longer distance along the x-axis per unit of time, reflecting faster movement. In contrast, steeper trajectory segments suggest that individuals spent more time on this journey, which could potentially indicate congestion. In all scenarios, both the blue and red spatial and temporal trajectories exhibit a "gentle-steep-gentle" pattern, corresponding to the three phases of entering the corridor, in the corridor and leaving the corridor, respectively. It is indicated that participants experienced a sequence of rapid walking, congestion, and then resumed rapid walking, particularly noticeable in the connecting corridor area where the steep trajectory is prominent. However, it is essential to note that the extent and duration of these steeper trajectory segments increased as the heeling angle increased. This phenomenon indicates that heeling scenarios not only had a substantial impact on human free speed but also worsened congestion.

To gain deeper insights into the human movement dynamics within the connecting corridor area, it is imperative to conduct a quantitative analysis of density. The conventional approach to calculate density is typically used to divide the number of individuals in a given area by its size. However, this method is often influenced by both the number of people and their spatial distribution. Therefore, it typically serves as the foundation for verifying macro pedestrian flow models and is not directly applicable to micro-level analyses (Zhang et al., 2011). In this study, the Voronoi method is employed to calculate people density at each frame, a technique that significantly improves the accuracy and applicability of density statistics evident by literatures (Hu et al., 2023; Liao et al., 2016), as depicted in Fig. 10. In this approach, each participant within the measurement area is treated as a sample point for a Thiessen Polygon. The fluctuation of density calculated by Voronoi method is more detailed, and the results are in better agreement. The density of each participant is evenly distributed into their respective polygon, resulting in the creation of a Thiessen Polygon diagram (Zhang et al., 2011). Fig. 10 provides an example of Thiessen Polygon demarcation for a corridor area containing 17 pedestrians. The specific Voronoi method is employed to calculate the density contribution of each participant to the Thiessen Polygon, as well as the average density of the measurement area, as illustrated in Equations (2) and (3) (Liao et al., 2016):

$$\rho_i(x, y) = \begin{cases} \frac{1}{S_v(i)} : (x, y) \in S_v \\ 0 : \text{otherwise} \end{cases} \quad (2)$$

$$\rho(t) = \frac{\int_{S_v} \sum_i \rho_i(x, y) dS_v(i)}{S_v} \quad (3)$$

where,  $\rho_i(x, y)$  is the density of individual  $i$  coordinates  $(x, y)$ , which is



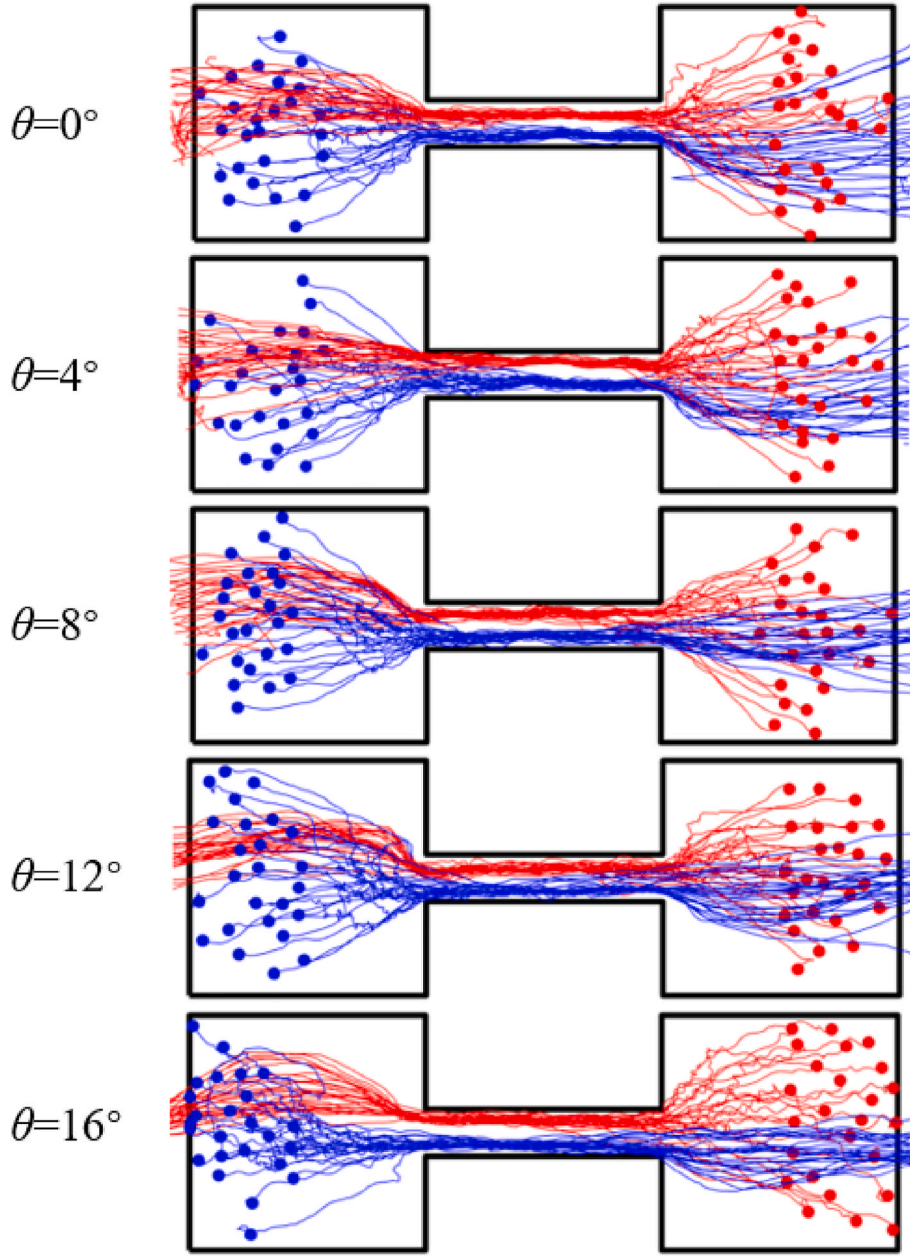


Fig. 8. Trajectories of all counterflow tests. Circles represent the initial positions of participants.

the reciprocal of the area  $S_v(i)$  of its Thiessen Polygon.  $\rho(t)$  is the average density of the measurement area at moment  $t$ , and  $S_v$  is the area of the entire measurement space.

During the process of employing this method to calculate density, the initial step involves accurately determining whether the coordinates of each participant fall within the designated density calculation area. Upon confirming that participant  $i$  is located in this area, the local density  $\rho_i(x, y)$  corresponding to participant  $i$  is calculated using Equation (2), based on the Tyson polygon area allocation principle. Subsequently, the average density  $\rho(t)$  of the measurement area at time  $t$  is derived through integral calculation using Equation (3).

It is illustrated that the trend of participant density in the corridor over time across various heeling scenarios in Fig. 11. In general, as participants first enter the corridor, the overall density gradually increases until the corridor area becomes saturated with individuals, causing the density curve to exhibit fluctuations. As most participants pass through the corridor, the density values in all heeling scenarios

commence a decline. To reduce the interference of density analysis caused by the increasing density phase when individuals begin entering the corridor and the decreasing density phase when they exit the corridor, it is found that when the time ranges from 10 to 20 s, the density in all heeling scenarios reached to stable stage, which is highlighted by the shaded part in Fig. 11.

The density of participants during this phase is shaded in Fig. 11. It is indicated that when the heeling angle reaches  $16^\circ$ , the density in the corridor is notably lower than in other scenarios. This phenomenon may be attributed to individuals' preference for maintaining more personal space to avoid overcrowding in this specific heeling scenario, and a similar finding was reported in the literature (Murayama et al., 2000). However, at heeling angle of  $4^\circ$  or  $8^\circ$ , the density is slightly higher than in scenarios with no heeling. This could be due to the fact that in both scenarios, the heeling condition generated a heightened urgency to complete evacuation promptly, resulting in increased competitive behaviour among participants to traverse the corridor area swiftly.

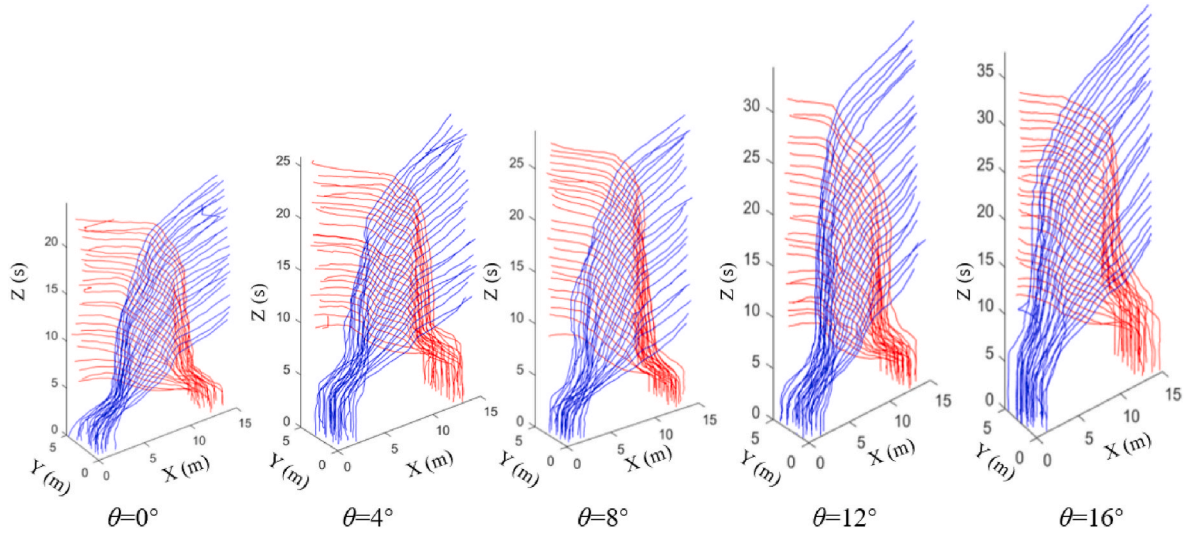


Fig. 9. The 3D trajectories at different heeling angles.

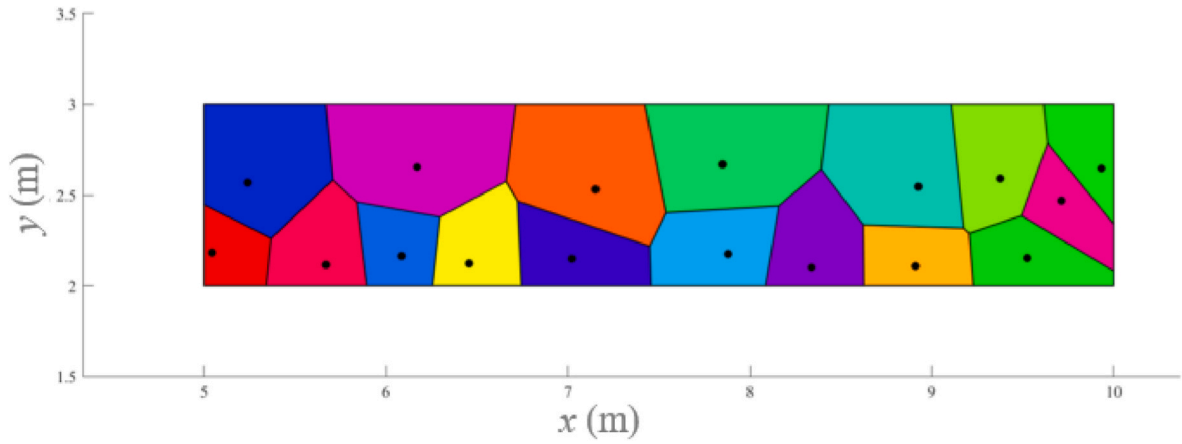


Fig. 10. The population density is calculated by Voronoi diagram method.

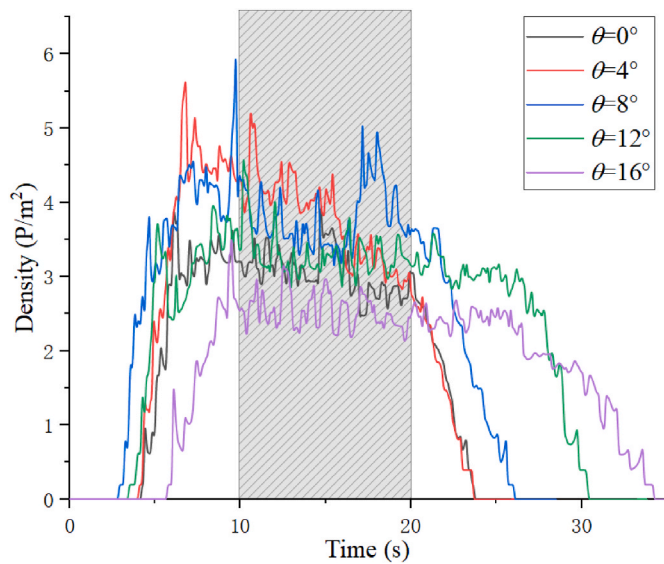


Fig. 11. The density curve in the connection area at different heeling angles.

Moreover, the speeds of participants in these two scenarios remained relatively unaffected, leading to higher corridor density due to the concentration of participants within this area. However, when the heeling angle is  $12^\circ$ , the density in this scenario is comparable to that of the no-heeling scenario. It is suggested that with a heeling angle of  $12^\circ$ , individuals make a trade-off between maintaining their speed and avoiding overcrowding.

To provide a clearer depiction of the evacuation process when the corridor area reaches a stable density level, Fig. 12 presents heat maps of participant density on the experimental simulator at various heeling angles at evacuation times  $t = 10, 15$ , and  $20$  s. At  $10$  s into the evacuation, a heightened density is observed connecting the two entrances of the corridor, indicating a significant number of individuals queuing up to traverse the corridor at this point. Notably, as the heeling angle increases, density in the corridor gradually diminishes, while the area of the high-density region forming at the two entrances of the corridor gradually expands. It is indicated that heeling angles intensify congestion at both corridor entrances. By the  $15$  s mark, in scenarios with heeling angles of  $0^\circ$  and  $4^\circ$ , the high-density crowd at both corridor entrances has largely dispersed. At this point, participants who have yet to complete evacuation primarily gather within the corridor area, resulting in high-density areas primarily occurring within the corridor. However, in scenarios with heeling angles of  $8^\circ$ ,  $12^\circ$ , and  $16^\circ$ , high-density areas still exist at both corridor entrances, but their size is

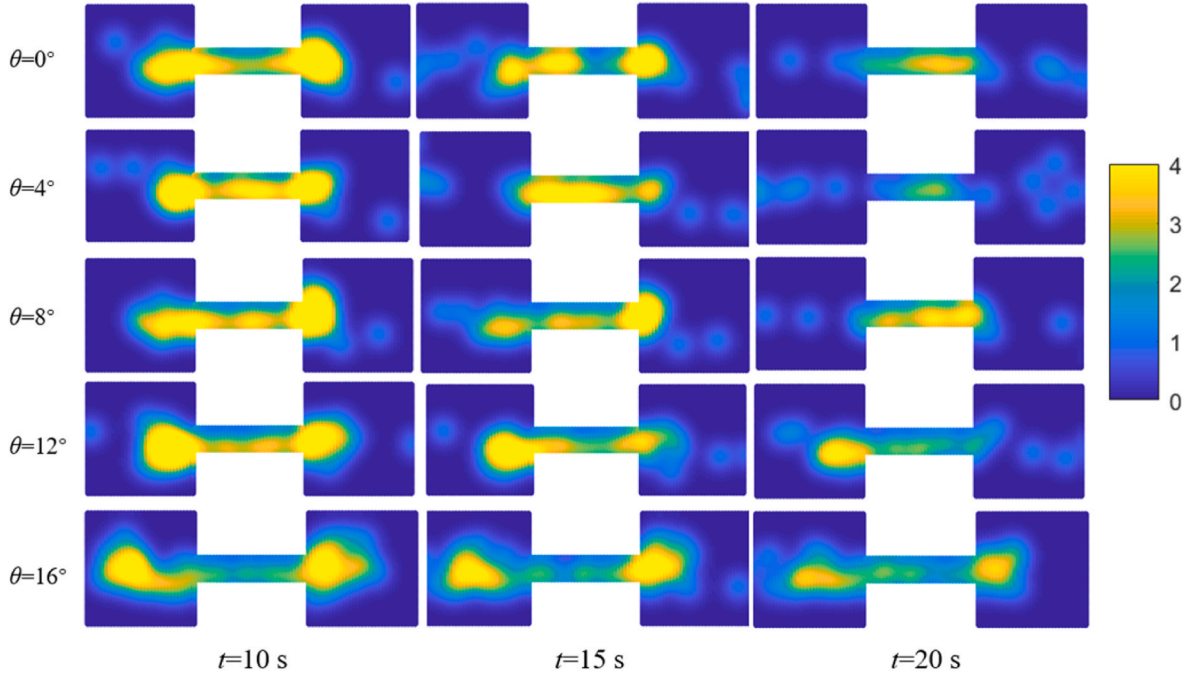


Fig. 12. Heat map of evacuation simulator density when  $t = 10$  s,  $15$  s, and  $20$  s.

significantly reduced compared to the 10 s evacuation mark. When the evacuation time reaches 20 s, most participants in all scenarios, except those with heeling angles of  $12^\circ$  and  $16^\circ$ , have already left the experimental simulator, and high-density areas are no longer present at both corridor entrances. It is indicated that the greater the heeling angle, the longer people experience congestion in the narrow area. In the scenario with a heeling angle of  $12^\circ$ , high-density areas appear only on one side. The possible reason is that the movement pattern observed when people walk in the opposite direction of a crowd often depends on the speed of the lead person (Hu et al., 2019). That is, the faster the initial person, the quicker all followers in the same direction behind them may pass through the intersection area of the opposing flow of people. In contrast, in the scenario with a heeling angle of  $16^\circ$ , individuals are still waiting to be evacuated at both corridor entrances, signifying that as the heeling angle increases, the time it takes for people to pass through the corridor area lengthens, exacerbating congestion during evacuation.

Human density serves as an indicator of the level of congregation at a specific point in time but cannot directly depict evacuation efficiency. In the realm of pedestrian dynamics, fundamental diagrams involving the density-speed relationship and density-flow relationship are commonly employed as pivotal quantitative assessment tools for evaluating evacuation systems (Li et al., 2023; Liao et al., 2016). Therefore, it becomes essential to incorporate parameters like the instantaneous speed of participants and the number of individuals passing through a given cross-section per unit time, denoted as the flow rate, to quantitatively characterize human movement features throughout the evacuation process. The calculation of instantaneous speed and flow rate is detailed in Equations (4) and (5) (Hu et al., 2023):

$$v_i = \frac{\sqrt{(P_i(t + \Delta t/2) - P_i(t - \Delta t/2))^2}}{\Delta t} \quad (4)$$

$$J_s(t) = \rho(t) \times v(t) \quad (5)$$

where,  $P_i(t)$  denotes the position of individual  $i$  at time  $t$ ,  $\Delta t$  is the time interval between two positions, and  $\Delta t$  takes the value of 0.4 s in this work;  $\rho(t)$  and  $v(t)$  denote the average density and the average speed of individuals in the area at time  $t$ , respectively.

To clarify the intricate relationship between density and speed dur-

ing human evacuation at varying heeling angles, the fundamental diagrams of human density and walking speed under different heeling angles are presented in Fig. 13. Furthermore, to visually describe the functional relationship between density and speed in various heeling scenarios, Equation (6) employs an exponential function for nonlinear data fitting of density and speed. The objective of fitting walking speed and density is to provide a clearer understanding of the real-time speed-density relationship at different heeling angles, aiding in the comprehension of speed corresponding to the density determined in various heeling scenarios. Moreover, these foundational speed-density maps offer a concise quantitative validation for subsequent relevant studies.

$$v(\rho) = a \times \exp(-b\rho) + c \quad (6)$$

where,  $v(\rho)$  is the average speed when the density is  $\rho$ .  $a$ ,  $b$  and  $c$  are constants of the fitting function, which determine the trend of the function curve. The specific values of them are shown in Table 3.

In all experimental scenarios, the density-speed relationship consistently demonstrates a noticeable pattern of decreasing velocity as density increases. Nevertheless, it is crucial to emphasize that there are notable distinctions in human movement speed across various heeling angles. Larger heeling angles typically correspond to lower human moving speeds, particularly at higher densities. However, once the density reaches  $4 \text{ P/m}^2$ , individuals tend to come to a halt regardless of the heeling angles. Therefore, the variability in velocity is minimal at this juncture.

Furthermore, in scenarios with heeling angles of  $0^\circ$  and  $4^\circ$ , the distribution of density and speed exhibits relatively uniform patterns, with no apparent clustering of data points. However, as the heeling angle increases to  $8^\circ$ , a substantial number of data points start to concentrate within the density range of  $[3.2, 4.5] \text{ P/m}^2$ , as illustrated by the blue data points in Fig. 13. With further increases in the heeling angle, this concentration gradually diminishes and becomes centred within the density ranges of  $[2.8, 3.6] \text{ P/m}^2$  and  $[1.7, 2.7] \text{ P/m}^2$  in the  $12^\circ$  and  $16^\circ$  scenarios, respectively. It is suggested that heightened heeling angles not only lead to a reduction in human movement speed but also curtail the formation of large-scale crowds. Consequently, individuals tend to favour completing their evacuation in relatively low-density environments. It is reflected that a heightened desire for a larger personal space



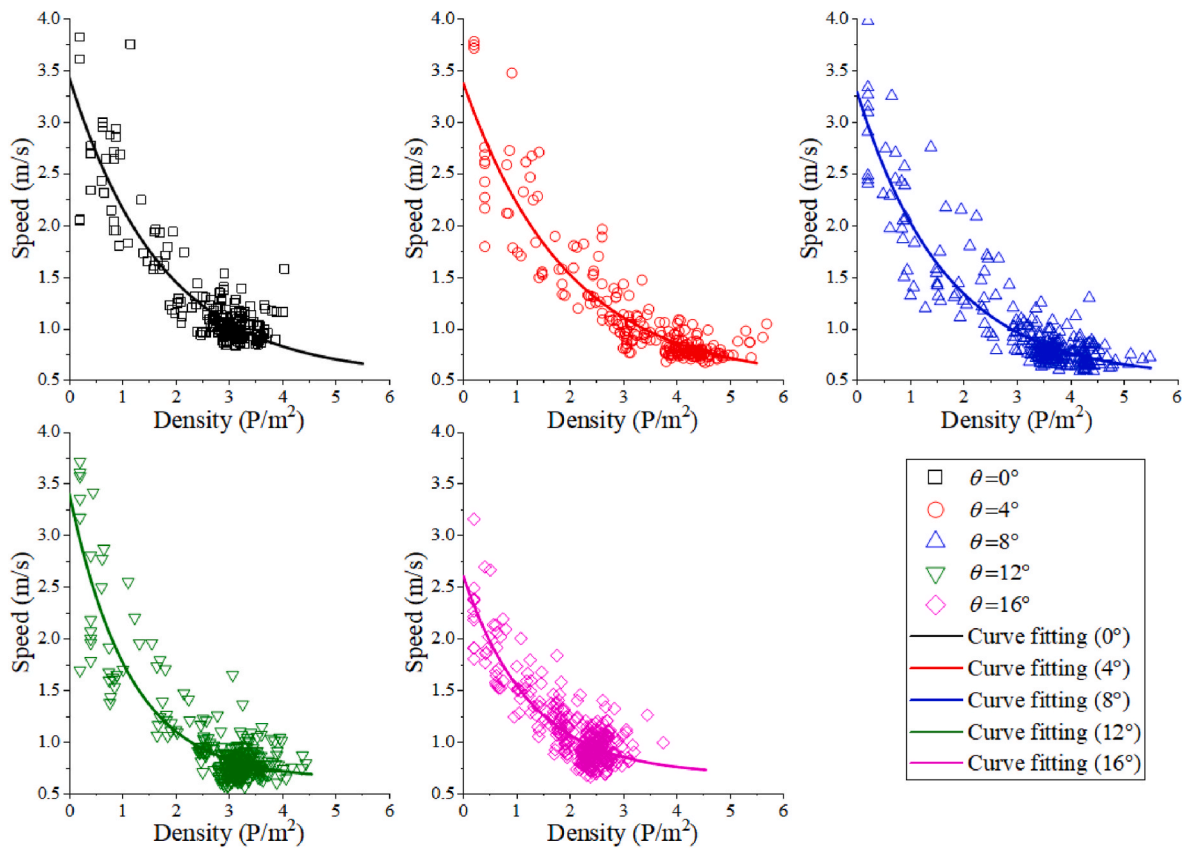


Fig. 13. Density-speed fundamental diagram at different heeling angles.

Table 3

The coefficient values of the fitting functions.

	a	b	c
$\theta = 0^\circ$	2.885	0.5775	0.5448
$\theta = 4^\circ$	2.874	0.5156	0.5008
$\theta = 8^\circ$	2.761	0.6118	0.5275
$\theta = 12^\circ$	2.761	0.8962	0.6479
$\theta = 16^\circ$	1.921	0.7995	0.6862

to facilitate adjustments in their maneuvers on heeling ships, and this desire increases with escalating heeling angles.

The density-flow fundamental diagrams for each heeling scenario are analysed to offer a more visual comparison of the impact of different heeling angles, as depicted in Fig. 14. A linear fit is conducted, and 95% prediction bands with light-coloured areas are delineated in Fig. 14. In general, it is observed that the flow rate continued to rise as the density increased in all scenarios. While some studies emphasize that the flow rate stabilizes beyond a certain density threshold and does not continue to increase (Hu et al., 2023; Li et al., 2023), this phenomenon was not observed in this study. It may be attributed to specific focus on the connecting corridor of the experimental simulator, excluding the high-density areas at both entrances of the corridor, as previously mentioned. Furthermore, this study focused on the evacuation process for opposite walking directions, wherein both entrances of the corridor allowed free access for participants. This might have resulted in a density threshold that led to a stabilized flow value, which exceeded the possible actual observation in this counter flow test. However, the flow patterns align with the conclusions drawn from the investigation of opposite-direction pedestrian flows conducted by Wang et al. (2019).

In addition, with an increase in the heeling angle, the flow rate at the same density diminishes. For instance, in the scenario with a heeling angle of  $16^\circ$ , the average flow rate is merely  $1.25 \text{ P/(m}\cdot\text{s)}$  when the

density is  $3 \text{ P/m}^2$ . This represents a decrease of approximately 20.1% compared to the values of  $1.58 \text{ P/(m}\cdot\text{s)}$  observed in the scenarios with no heeling. It is highlighted that the reduction in human evacuation efficiency and flow rate as the heeling angle intensifies, which can offer valuable insights for shaping evacuation strategies and enhancing safety management during ship heeling events.

#### 4.4. Discussion

The experimental findings in this study convincingly illustrate that heeling ships can significantly impact human evacuation, with different heeling angles exerting varying yet generally negative effects on human movement. Compared to the previous studies in the field, it reveals new findings in a more quantitative manner, indicating the exact effect of different angles on the evacuation. It therefore provides new and unique contributions on the improved measures for the evacuation on passenger ships. Specifically, it is advisable for managers to consider the characteristics of human movement on heeling ships during emergency evacuation. Conducting timely ship condition assessments and having a clear understanding of the optimal timeframe for human evacuation are crucial to prevent severe heeling angles from impeding the evacuation process. When evacuation activities have to be carried out at a large heeling angles ( $>10^\circ$ ), the managers should fully consider the negative impact of such scenarios on the human movement, and take more protective measures and provide more attention to the passengers as much as possible (Wang et al., 2023b). Although the participants recruited for this study may not entirely represent the diversity of all passengers on board, their demonstrated speed attenuation trend in the heeling scenarios essentially reflects the general behavioural pattern of most normal passengers. However, it's worth noting that older or less mobility passengers may encounter more pronounced challenges and potential risks when the ship experiences significant heeling angles. Therefore, ship managers should prioritize the needs and safety of these



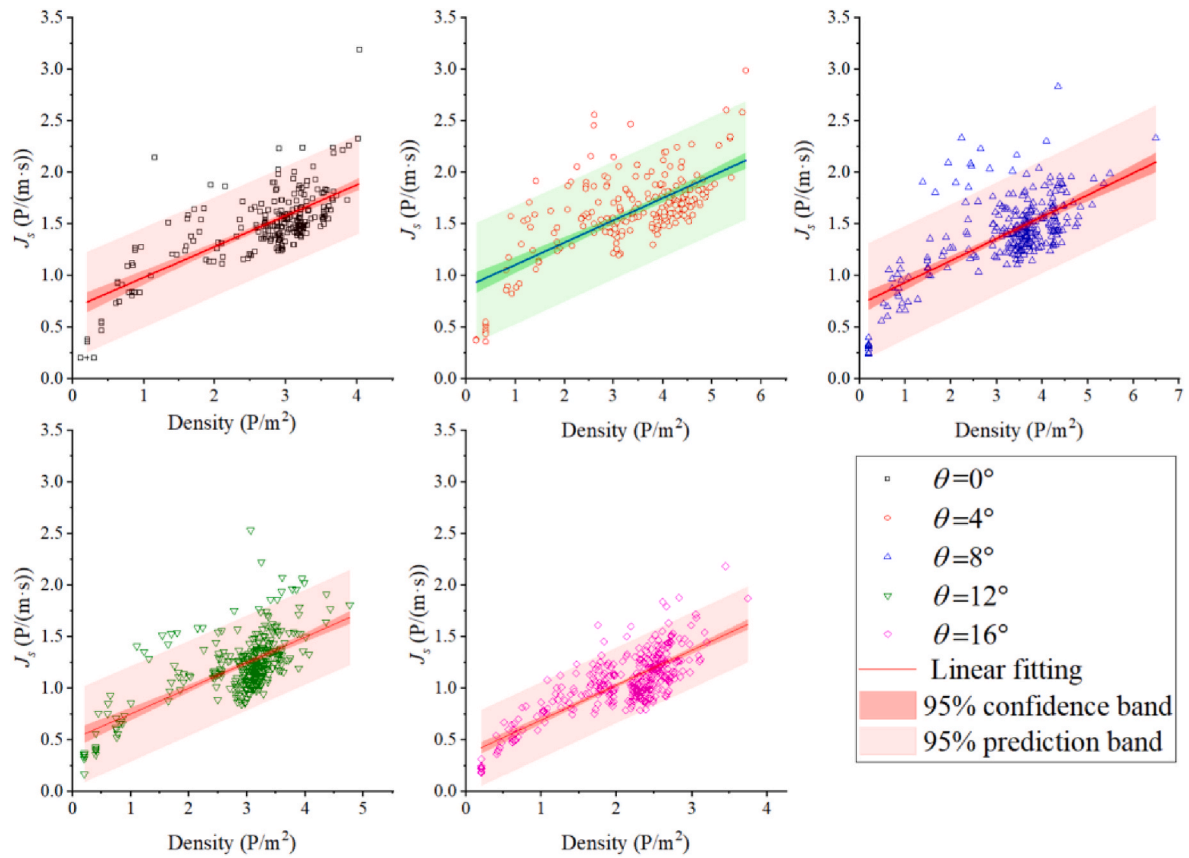


Fig. 14. Density-flow rate fundamental diagrams at different heeling angles.

passengers, ensuring that necessary assistance and support can be promptly provided to them in case of emergencies.

Additionally, it is evident that heeling ships prolong the duration of complete evacuation experiments while diminishing human movement speed, which can be exemplified by the increased congestion in narrow passage areas with escalating heeling angles. Therefore, managers should organize on-board human evacuations systematically and offer appropriate guidance services for individuals unfamiliar with the ship's layout to prevent overcrowding due to herd behaviour (Fang et al., 2022b). Furthermore, compared to scenarios with no heeling, it becomes evident that people require more space to adjust their movements to accommodate the heeling ship. This results in a reduction in people density as heeling angles increase, subsequently leading to a decrease in the flow rate within the measurement area. These metrics can serve as indicative data for assessing the efficiency of evacuating people from a ship.

Understanding the movement characteristics of individuals and crowd behaviour in heeling ships is foundational for successful human evacuation in emergencies. However, due to concerns about experimental safety, most current experimental setups primarily focus on the movement of single individuals or single columns of individuals, and complete evacuation experiments cannot be carried out. It can be difficult to accurately quantify the impact of heeling ships on the movement of a single individual, and this may not fully represent the performance and characteristics of individuals during a comprehensive evacuation. This limitation can lead to conclusions in such studies, while still holding some reference value, having a considerable margin of error when compared to real-world scenarios (Galea et al., 2013; Kim et al., 2019). Therefore, recognizing that the experiments carried out here encompassed a typical scenario recommended by the IMO guidelines, this study examined two modes of movement speeds while for the first time, embedding the counter flow analysis in systematical analysis of

human evacuation performance in various heeling scenarios. These findings can offer valuable insights for ship managers as they develop evacuation strategies for future emergencies. Additionally, they can stimulate further contemplation for future research on human evacuation aboard ships.

Due to the constraints of experimental costs, obtaining and analysing evacuation data in heeling scenarios on full-size ships is impractical. However, contemporary simulation technology has advanced considerably, leading to the development and application of more sophisticated evacuation models in the field of human evacuation onboard ships (Cotfas et al., 2023; Fang et al., 2022a). These models can serve as a viable alternative to compensate for the limitations of conducting evacuation experiments in such scenarios. Nonetheless, it is important to emphasize that constructing these models still requires a robust foundation based on real-world experimental data. The findings of this study can offer essential validation for human evacuation, encompassing both individual speed and counter flow evacuation. This validation serves to enhance the reliability and accuracy of model simulations, thus facilitating the development of subsequent full-size or large-scale simulations of human evacuation aboard ships in extreme scenarios (Galea et al., 2012; Yue et al., 2022).

## 5. Conclusion

To comprehensively analyse the evacuation performance of individuals in heeling ships, an experimental simulator that closely aligns with the IMO's recommended scenario was established. Using video tracking technology, this work conducted tests on human free speeds and carried out counter flow evacuation. These experiments not only reveal the characteristic aspects of human movement in heeling situations but also quantitatively assess the connection between critical factors like speed, density, and flow rate during counter flow crowd

evacuation and the angle of heeling.

During the human free speed tests, participants' walking and running speeds were separately calculated. It is observed that a substantial decrease in human speed with an increase in the heeling angle. Notably, when the heeling angle reached 16°, both walking and running speeds exhibited a considerable reduction, with an average deceleration of 18.3% and 27.8%, respectively. Furthermore, the analysis of the relationship between participants' walking speed and their height in various heeling scenarios revealed that human walking and running speeds exhibited a linear increase with height. The findings indicated that males achieve higher walking and running speeds compared to females at the same heeling angles. Notably, in scenarios with a 16° heeling angle, males exhibited significantly less deceleration in speed than females. This suggests that among all participants in this experiment, males demonstrate greater adaptability to the heeling environment, enabling them to effectively adjust and sustain relatively higher speeds.

In the counter flow experiments, particular emphasis is placed on understanding the impact of different heeling scenarios on complete evacuation. The results clearly demonstrate that heeling scenarios significantly increase evacuation times. Specifically, a heeling angle of 16° resulted in a substantial 52.8% increase in evacuation time. Upon conducting a quantitative analysis of crowd evacuation in the intersection area (corridor), it is observed that there was no significant reduction in human speed at heeling angles of 4° and 8°. However, the density in the corridor area was higher compared to the no-heeling case, indicating that people were more eager to complete evacuation in these scenarios. Conversely, when the heeling angle reached 16°, human speed decreased significantly, leading to a pronounced reduction in corridor area density. Furthermore, the calculations of the flow rate in the corridor area revealed that the flow rate increased with higher densities. Nevertheless, increasing heeling angles had a decreasing effect on the overall flow rate. In fact, at a heeling angle of 16°, the overall flow rate decreased by approximately 20.1% compared to the no-heeling scenario. This underscores the negative impact of heeling scenarios on human evacuation efficiency aboard ships.

The conclusions drawn from this study have significant implications for enhancing the understanding of human evacuation characteristics during ship heeling scenarios. The data collected can offer both qualitative and quantitative validation for future human evacuation models, thereby enhancing the accuracy and comprehensibility of full-size human evacuation simulations for passenger ships. However, this study has certain limitations due to experimental conditions. Firstly, the study involved only healthy students aged 18–25, which may not represent the diversity of age groups found in the actual shipboard population. Secondly, the experiment was restricted to a maximum heeling angle of 16° for safety reasons, leaving larger angles unexplored. The experimental scenario took place on an open platform, and while efforts were made to simulate ship heeling as accurately as possible, the impact of ship interior features such as walls and handrails on human evacuation was not fully considered. Finally, the panic emotion of the participants has yet been taken into account. Future research may explore alternative methods, such as virtual reality, to collect additional data on human movement parameters and emergency evacuation behaviours, thus contributing to enhanced passenger ship safety.

#### CRedit authorship contribution statement

**Siming Fang:** Writing – original draft, Validation, Methodology, Investigation, Conceptualization. **Zhengjiang Liu:** Validation, Supervision, Project administration. **Xinjian Wang:** Resources, Funding acquisition, Formal analysis, Conceptualization. **Ben Matellini:** Writing – original draft, Validation, Formal analysis. **Jin Wang:** Validation, Supervision, Resources. **Zaili Yang:** Writing – review & editing, Validation, Supervision, Formal analysis. **Xinyu Zhang:** Project administration, Conceptualization. **Bo Wan:** Project administration. **Shengke Ni:** Funding acquisition, Visualization, Writing – review & editing.

#### Declaration of competing interest

The authors declare that they have no known competing financial interests or personal relationships that could have appeared to influence the work reported in this paper.

#### Data availability

Data will be made available on request.

#### Acknowledgements

The authors gratefully acknowledge support from the National Natural Science Foundation of China (Grant No. 52101399; 52301409), Ministry of Industry and Information Technology Joint Equipment (Grant No. 2019[357]), Bolian Research Funds of Dalian Maritime University (Grant No. 3132023617). This work is also financially supported by European Research Council project (TRUST CoG 2019 864724).

#### References

- Arshad, H., Emblemavåg, J., Li, G., et al., 2022. Determinants, methods, and solutions of evacuation models for passenger ships: a systematic literature review. *Ocean Eng.* 263, 112371 <https://doi.org/10.1016/j.oceaneng.2022.112371>.
- Azizpour, H., Galea, E.R., Erland, S., et al., 2022. An experimental analysis of the impact of thermal protective immersion suit and angle of heel on individual walking speeds. *Saf. Sci.* 152, 105621 <https://doi.org/10.1016/j.ssci.2021.105621>.
- Bartolucci, A., Casareale, C., Drury, J., 2021. Cooperative and competitive behaviour among passengers during the costa concordia disaster. *Saf. Sci.* 134, 105055 <https://doi.org/10.1016/j.ssci.2020.105055>.
- Bles, W., Nooy, S., Boer, L.C., 2001a. Influence of ship listing and ship motion on walking speed. In: *Conference on Pedestrian and Evacuation Dynamics (PED 2001)*. Springer, Berlin, p. 437.
- Bles, W., Nooy, S., Boer, L.C., 2001b. Influence of Ship Listing and Ship Motion on Walking Speed. Springer, p. 437.
- Browne, T., Taylor, R., Veitch, B., et al., 2022. A general method to combine environmental and life-safety consequences of Arctic ship accidents. *Saf. Sci.* 154, 105855 <https://doi.org/10.1016/j.ssci.2022.105855>.
- Browne, T., Veitch, B., Taylor, R., et al., 2021. Consequence modelling for Arctic ship evacuations using expert knowledge. *Mar. Pol.* 130, 104582 <https://doi.org/10.1016/j.marpol.2021.104582>.
- Brumley, A., Koss, L.J.P.o.A., 1998. *The Implication of Human Behavior on the Evacuation of Ferries and Cruise Ships*, vol. 98.
- Cao, Y., Wang, X., Wang, Y., et al., 2023a. Analysis of factors affecting the severity of marine accidents using a data-driven Bayesian network. *Ocean Eng.* 269, 113563 <https://doi.org/10.1016/j.oceaneng.2022.113563>.
- Cao, Y.H., Wang, X.J., Yang, Z.L., et al., 2023b. Research in marine accidents: a bibliometric analysis, systematic review and future directions. *Ocean Eng.* 284, 115048 <https://doi.org/10.1016/j.oceaneng.2023.115048>.
- Chan, J.P., Pazouki, K., Norman, R.A., 2023. An experimental study into the fault recognition of onboard systems by navigational officers. *J. Mar. Eng. & Technol.* 22, 101–110. <https://doi.org/10.1080/20464177.2022.2143312>.
- Chang, C.-H., Stergiou, N., Kaipust, J., et al., 2015. Walking before and during a sea voyage. *Ecol. Psychol.* 27, 87–101. <https://doi.org/10.1080/10407413.2015.991656>.
- Christensen, M., Georgati, M., Arsanjani, J.J., 2022. A risk-based approach for determining the future potential of commercial shipping in the Arctic. *J. Mar. Eng. & Technol.* 21, 82–99. <https://doi.org/10.1080/20464177.2019.1672419>.
- Cotfas, L.-A., Delcea, C., Mancini, S., et al., 2023. An agent-based model for cruise ship evacuation considering the presence of smart technologies on board. *Expert Syst. Appl.* 214, 119124 <https://doi.org/10.1016/j.eswa.2022.119124>.
- Eliopoulou, E., Alissafaki, A., Papanikolaou, A., 2023. Statistical analysis of accidents and review of safety level of passenger ships. *J. Mar. Sci. Eng.* 11, 410. <https://doi.org/10.3390/jmse11020410>.
- Fang, S., Liu, Z., Wang, X., et al., 2024. Dynamic analysis of emergency evacuation in a rolling passenger ship using a two-layer social force model. *Expert Syst. Appl.* 247, 123310 <https://doi.org/10.1016/j.eswa.2024.123310>.
- Fang, S., Liu, Z., Wang, X., et al., 2022a. Simulation of evacuation in an inclined passenger vessel based on an improved social force model. *Saf. Sci.* 148, 105675 <https://doi.org/10.1016/j.ssci.2022.105675>.
- Fang, S., Liu, Z., Yang, X., et al., 2023. A quantitative study of the factors influencing human evacuation from ships. *Ocean Eng.* 285, 115156 <https://doi.org/10.1016/j.oceaneng.2023.115156>.
- Fang, S., Liu, Z., Zhang, S., et al., 2022b. Evacuation simulation of an Ro-Ro passenger ship considering the effects of inclination and crew's guidance. *Proc. IME M J. Eng. Marit. Environ.* 237, 192–205. <https://doi.org/10.1177/14750902221106566>.

- Galea, E.R., Deere, S., Brown, R., et al., 2013. An experimental validation of an evacuation model using data sets generated from two large passenger ships. *J. Ship Res.* 57, 155–170. <https://doi.org/10.5957/JOSR.57.3.120037>.
- Galea, E.R., Grandison, A., Blackshields, D., et al., 2012. IMO INF Paper Summary-The SAFEGUARD Enhanced Scenarios and Recommendations to IMO to Update MSC Circ 1238.
- Hu, Y., Bi, Y., Ren, X., et al., 2023. Experimental study on the impact of a stationary pedestrian obstacle at the exit on evacuation. *Phys. Stat. Mech. Appl.* 626, 129062 <https://doi.org/10.1016/j.physa.2023.129062>.
- Hu, Y.H., Zhang, J., Song, W.G., 2019. Experimental study on the movement strategies of individuals in multidirectional flows. *Phys. Stat. Mech. Appl.* 534, 122046 <https://doi.org/10.1016/j.physa.2019.122046>.
- Huang, D.Z., Liang, T.T., Hu, S.P., et al., 2023. Characteristics analysis of intercontinental sea accidents using weighted association rule mining: evidence from the Mediterranean Sea and Black Sea. *Ocean Eng.* 115839 <https://doi.org/10.1016/j.oceaneng.2023.115839>.
- Hwang, K., 2013. An experiment on walking speeds of freshmen unexperienced in shipboard life on a passenger ship. *J. Navigation and Port Res.* 37, 239–244.
- IMO, 2016. Revised Guidelines for Evacuation Analysis for New and Existing Passenger Ships. IMO MSC.1/Circ 1533, 6 June 2016.
- Kang, Z., Zhang, L., Li, K., 2019. An improved social force model for pedestrian dynamics in shipwrecks. *Appl. Math. Comput.* 348, 355–362. <https://doi.org/10.1016/j.amc.2018.12.001>.
- Kim, H., Haugen, S., Utne, I.B., 2016. Assessment of accident theories for major accidents focusing on the MV SEWOL disaster: similarities, differences, and discussion for a combined approach. *Saf. Sci.* 82, 410–420. <https://doi.org/10.1016/j.ssci.2015.10.009>.
- Kim, H., Roh, M.-I., Han, S., 2019. Passenger evacuation simulation considering the heeling angle change during sinking. *Int. J. Nav. Archit. Ocean Eng.* 11, 329–343. <https://doi.org/10.1016/j.ijnaoe.2018.06.007>.
- Kimera, D., Nangolo, F.N., 2022. Reliability maintenance aspects of deck machinery for ageing/aged fishing vessels. *J. Mar. Eng. & Technol.* 21, 100–110. <https://doi.org/10.1080/20464177.2019.1663595>.
- Koss, L., Moore, A., Porteous, B., 1997. Human mobility data for movement on ships. In: *International Conference on Fire at Sea*, pp. 11–21. London.
- Lee, D., Park, J.-H., Kim, H., 2004. A study on experiment of human behavior for evacuation simulation. *Ocean Eng.* 31, 931–941. <https://doi.org/10.1016/j.oceaneng.2003.12.003>.
- Li, H., Zhang, J., Song, W., 2023. A comparative experimental study on the influence of bottleneck width on evacuation characteristics of pedestrian flow in funnel shape bottleneck and normal bottleneck. *Phys. Stat. Mech. Appl.* 624 <https://doi.org/10.1016/j.physa.2023.128929>.
- Liao, W., Tordeux, A., Seyfried, A., et al., 2016. Measuring the steady state of pedestrian flow in bottleneck experiments. *Phys. Stat. Mech. Appl.* 461, 248–261. <https://doi.org/10.1016/j.physa.2016.05.051>.
- Liu, D., Rong, H., Guedes Soares, C., 2023. Shipping route modelling of AIS maritime traffic data at the approach to ports. *Ocean Eng.* 289, 115868 <https://doi.org/10.1016/j.oceaneng.2023.115868>.
- Liu, K., Ma, Y., Chen, M., et al., 2022. A survey of crowd evacuation on passenger ships: recent advances and future challenges. *Ocean Eng.* 263, 112403 <https://doi.org/10.1016/j.oceaneng.2022.112403>.
- Murayama, M., Itagaki, T., Yoshida, K., 2000. Study on evaluation of escape route by evacuation simulation escape in listed ship. *J. Soc. Nav. Archit. Jpn.* 2000, 441–448.
- Rong, H., Teixeira, A.P., Soares, C.G., 2022a. Maritime traffic probabilistic prediction based on ship motion pattern extraction. *Reliab. Eng. Syst. Saf.* 217, 108061 <https://doi.org/10.1016/j.res.2021.108061>.
- Rong, H., Teixeira, A.P., Soares, C.G., 2022b. Ship collision avoidance behaviour recognition and analysis based on AIS data. *Ocean Eng.* 245, 110479 <https://doi.org/10.1016/j.oceaneng.2021.110479>.
- Shafiee, M., Animah, I., 2022. An integrated FMEA and MCDA based risk management approach to support life extension of subsea facilities in high-pressure-high-temperature (HPHT) conditions. *J. Mar. Eng. & Technol.* 21, 189–204. <https://doi.org/10.1080/20464177.2020.1827486>.
- Sun, J., Guo, Y., Li, C., et al., 2018a. An experimental study on individual walking speed during ship evacuation with the combined effect of heeling and trim. *Ocean Eng.* 166, 396–403. <https://doi.org/10.1016/j.oceaneng.2017.10.008>.
- Sun, J., Lu, S., Lo, S., et al., 2018b. Moving characteristics of single file passengers considering the effect of ship trim and heeling. *Phys. Stat. Mech. Appl.* 490, 476–487. <https://doi.org/10.1016/j.physa.2017.08.031>.
- Valcalda, A., de Koningh, D., Kana, A., 2022. A method to assess the impact of safe return to port regulatory framework on passenger ships concept design. *J. Mar. Eng. & Technol.* 1–12. <https://doi.org/10.1080/20464177.2022.2031557>.
- Walter, H., Wagman, J.B., Stergiou, N., et al., 2016. Dynamic perception of dynamic affordances: walking on a ship at sea. *Exp. Brain Res.* 235, 517–524. <https://doi.org/10.1007/s00221-016-4810-6>.
- Walter, H.J., Li, R., Wagman, J.B., et al., 2019. Adaptive perception of changes in affordances for walking on a ship at sea. *Hum. Mov. Sci.* 64, 28–37. <https://doi.org/10.1016/j.humov.2019.01.002>.
- Wang, A., Li, L., Mei, S., et al., 2021a. Hermite interpolation based interval shannon-cosine wavelet and its application in sparse representation of curve. *Mathematics* 1. <https://doi.org/10.3390/math9010001>.
- Wang, H., Liu, S., Wang, X., et al., 2021b. An analysis of factors affecting the severity of marine accidents. *Reliab. Eng. Syst. Saf.* 210, 107513 <https://doi.org/10.1016/j.res.2021.107513>.
- Wang, X., Zhou, L., Zhuang, L., et al., 2023a. A model of maritime accidents prediction based on multi-factor time series analysis. *J. Mar. Eng. & Technol.* 22, 153–165. <https://doi.org/10.1080/20464177.2023.2167269>.
- Wang, P., Cao, S., Yao, M., 2019. Fundamental diagrams for pedestrian traffic flow in controlled experiments. *Phys. Stat. Mech. Appl.* 525, 266–277. <https://doi.org/10.1016/j.physa.2019.03.057>.
- Wang, X., Liu, Z., Loughney, S., et al., 2021c. An experimental analysis of evacuees' walking speeds under different rolling conditions of a ship. *Ocean Eng.* 233, 108997 <https://doi.org/10.1016/j.oceaneng.2021.108997>.
- Wang, X., Liu, Z., Wang, J., et al., 2021d. Passengers' safety awareness and perception of wayfinding tools in a Ro-Ro passenger ship during an emergency evacuation. *Saf. Sci.* 137, 105189 <https://doi.org/10.1016/j.ssci.2021.105189>.
- Wang, X., Liu, Z., Zhao, Z., et al., 2020. Passengers' likely behaviour based on demographic difference during an emergency evacuation in a Ro-Ro passenger ship. *Saf. Sci.* 129, 104803 <https://doi.org/10.1016/j.ssci.2020.104803>.
- Wang, X., Xia, G., Zhao, J., et al., 2023b. A novel method for the risk assessment of human evacuation from cruise ships in maritime transportation. *Reliab. Eng. Syst. Saf.* 230, 108887 <https://doi.org/10.1016/j.res.2022.108887>.
- Xie, Q., Guo, S., Zhang, Y., et al., 2022. An integrated method for assessing passenger evacuation performance in ship fires. *Ocean Eng.* 262, 112256 <https://doi.org/10.1016/j.oceaneng.2022.112256>.
- Xie, Q., Wang, P., Li, S., et al., 2020. An uncertainty analysis method for passenger travel time under ship fires: a coupling technique of nested sampling and polynomial chaos expansion method. *Ocean Eng.* 195, 106604 <https://doi.org/10.1016/j.oceaneng.2019.106604>.
- Xin, X., Liu, K., Li, H., Yang, Z., 2024. Maritime traffic partitioning: An adaptive semi-supervised spectral regularization approach for leveraging multi-graph evolutionary traffic interactions. *Transportation Research Part C: Emerging Technologies* 164, 104670. <https://doi.org/10.1016/j.trc.2024.104670>.
- Yang, H., Cheng, X.D., Zhang, H.P., et al., 2014. Effect of right-hand traffic rules on evacuation through multiple parallel bottlenecks. *Fire Technol.* 50, 297–316. <https://doi.org/10.1007/s10694-013-0370-5>.
- Yue, Y., Gai, W.-m., Deng, Y.-f., 2022. Influence factors on the passenger evacuation capacity of cruise ships: modeling and simulation of full-scale evacuation incorporating information dissemination. *Process Saf. Environ. Protect.* 157, 466–483. <https://doi.org/10.1016/j.psep.2021.11.010>.
- Zhang, D.Z., Shao, N., Tang, Y., 2017. An evacuation model considering human behavior. In: *2017 IEEE 14th International Conference on Networking, Sensing and Control (ICNSC 2017)*, pp. 54–59.
- Zhang, J., Klingsch, W., Schadschneider, A., et al., 2011. Transitions in pedestrian fundamental diagrams of straight corridors and T-junctions. *J. Stat. Mech. Theor. Exp.* 2011, P06004 <https://doi.org/10.1088/1742-5468/2011/06/p06004>.